AD-A264 733

12

NSWCDD/TR-92/243

PHALANX CIWS CONTROL SYSTEM STABILITY, AIM BIAS COMPENSATION, AND NOISE SENSITIVITY

BY DEMETRIOS SERAKOS
COMBAT SYSTEMS DEPARTMENT

MAY 1992

DTIC
ELECTE
MAY 21 1993

Approved for public release; distribution is unlimited.

NAVAL SURFACE WARFARE CENTER
DAHLGREN DIVISION
Dahlgren, Virginia 22448-5000

93-11286

NSWCDD/TR-92/243

PHALANX CIWS CONTROL SYSTEM STABILITY, AIM BIAS COMPENSATION, AND NOISE SENSITIVITY

BY DEMETRIOS SERAKOS
COMBAT SYSTEMS DEPARTMENT

MAY 1992

Approved for public release; distribution is unlimited.

NAVAL SURFACE WARFARE CENTER
DAHLGREN DIVISION
Dahlgren, Virginia 22448-5000

FOREWORD

This report presents a stability analysis of an aiming control system that is similar to that used in the Block I PHALANX Close-In Weapon System (CIWS). Besides stability, other design goals of the control system are aim bias compensation and noise sensitivity. This report presents a theoretical analysis of these disparate goals and design tradeoffs are also presented. It is a continuation of previous work reported in Bailey, E.P. and Price E.L., *An Analysis of Gun Aim Bias Compensation for the PHALANX CIWS*, FMC Corporation, King George, Virginia, May 1987, which largely was an analysis of improved performance over a previous control system. Control theoretic issues such as stability, aim bias compensation and noise sensitivity were not considered in that work.

The author wishes to thank E.L. Price and M.H. Pee of FMC Corporation for introducing this subject and for their technical advice.

This report has been reviewed by A. Garza, Head, System Engineering Branch and R.E. Lutman, Head, AEGIS Ship Combat Systems Division.

Approved by:

L.M. Williams, III, Head
Combat Systems Department

Accession For
NTIS GRA&I
DTIC TAB
Unannounced
Justification
By
Distribution/
Availability Codes
Dist | Avail and/or Special
A-1

ABSTRACT

An aiming control system, which is similar to that in the Block I PHALANX Close In Weapon System is considered in this report. An important feature of this control system is that it compensates for any gun aim bias. An aim bias may be caused by variations in the gun, ammunition, or environmental conditions. Design issues considered are stability, aim bias compensation, and sensitivity to feedback noise. These are disparate design goals. Design tradeoffs that quantify this disparity are presented. An example is given that illustrates how the analysis developed in this report might be used in a design situation.

CONTENTS

ILLUSTRATIONS

INTRODUCTION

In this report an aiming control system that is similar to that in the Block I PHALANX Close-In Weapons System (CIWS) is considered. Among the important issues considered in designing this control system are stability, target tracking, disturbance rejection and sensitivity to noise. As it turns out, designing a system with better target tracking makes it less stable. Also, better target tracking makes the system more sensitive to noise. A system less susceptible to noise will be more susceptible to disturbances. Previously, no analytical work has been done quantifying these design considerations. The purpose of this report is to present an analytical picture to these design considerations that may be used to sharpen a current design or speed the development of a future design.

A broad picture of the problem is as follows: The desired gun aiming angle is fed into the control system. The aiming angle is treated as a reference input - the manner in which it is obtained is not considered in this report. The gun tracks this reference input. A proportional plus integral controller is used in an inner feedback loop to accomplish this. One problem is that there may be an aim bias. Among the factors contributing to an aim bias are: misalignment of the gun aiming mechanism, the barrels heating due to the gun being fired, barrel wear, variations in the propellant used, wind, temperature, and barrel warping due to sun load. The aim bias is modeled as a disturbance input. The control system features a second outer feedback loop to null out this bias. The bullet stream angle at the target is measured. Ideally, this stream should match the measured gun angle at the time those bullets were fired. If the two angles do not match, the error angle is fed back around the outer loop to compensate. The bullet stream angle measurement is noisy, so a noise filter is included in the outer feedback loop.

In the PHALANX CIWS Aiming Model section, a model for this system is defined and discussed. The transfer functions that are needed are computed. It will be seen that this is a linear sys-

tem with a time-varying time delay. Time delays are destabilizing. The time delay arises because the feedback to null out the aim bias involves past reference angles. The stability of the system is then considered. The first consideration is the stability of the inner loop. This part of the system is a linear system (with no time delays). The general, but conservative, Small-Gain Theorem[1], is used to give conditions for the closed-loop stability of the overall system. The Small-Gain Theorem applies to systems with time-varying time delays. Roughly speaking, the Small-Gain Theorem states that a feedback system is stable if the gain of the transfer functions around the feedback loop is less than one. In the Nyquist Stability With A Conjecture section, less conservative conditions for closed-loop stability are given, but a conjecture is needed.

Also in the PHALANX CIWS Aiming Model section, some design guidelines are given for disturbance rejection and sensitivity to noise. The disturbance is a perturbation on the system output. Hence, the disturbance is modeled as an addition to the system output. The noise acts to corrupt the measurement of the output signal. Hence, the noise is modeled as an addition in the outer feedback loop. Thus, the filter has two conflicting tasks. First, it should block off the sensor noise. At the same time it must not cut off the feedback loop too much because no information about the disturbance would be fed back, which is the point of the feedback loop. The idea is to observe that the frequency spectrum of the disturbance and noise are different. The disturbance has a low frequency spectrum, while the noise has a high frequency spectrum. Disturbances, such as aim bias, would be slowly varying. Noise, for instance, due to thermal effects on measurement sensors, would have a much higher frequency range. Thus, the desired filter is a low pass filter. The control design procedure used in this report is patterned after the theory developed in Fruedenberg–Looze[2].

An example is presented to illustrate how the stability conditions and performance measures, which are developed in this report, are used to design a satisfactory control system. The task of the designer is to select the proportional feedback gain, the integral feedback gain and the filter.

PHALANX CIWS AIMING MODEL

In this section, we discuss the model for the PHALANX gun, which is taken from Bailey–Price[3]. Figure 1 shows the angle geometry of the system. Figure 2 shows the timing diagram. In this diagram, the range of the bullet increases with time while the range of the target decreases with time. Figure 3 shows the block diagram for the system, using Laplace transform transfer functions. Following is a list of variables.

θ_a: Aim pointing angle (reference input)

θ_g: Measured gun angle

θ_b: Bullet angle at target

θ_d: Disturbance input

n: Measurement noise input

t_f: Bullet flight time (seconds)

$\hat{t}_f$: Estimated bullet flight time (seconds)

This is a one-dimensional model. In real life, there would be two angular channels, azimuth and elevation, but they would be independent of each other. The plant is modeled by a pure integrator. We use a proportional-integral (PI) controller, the gains are K_P and K_I. The derivative of θ_a is also a control input. This enables the gun to track inputs of a higher degree than step inputs; e.g., ramp inputs. There is an inner loop feeding back θ_g. This loop takes out any error of the gun aiming mechanism to the reference input. The outer loop, feeding back θ_b, takes out errors due to any disturbances. This includes, in particular, the gun aim bias (the gun aim bias is modeled as a disturbance). There is a time delay, because θ_b is the angle of the bullet stream at the target. The flight time of the bullets, t_f, is from the gun to the target. To get the gun aim bias, θ_b is compared to the expected bullet stream angle at the target, θ_g delayed by the estimated bullet flight time, $\hat{t}_f$. The goal of the filter, $F(s)$, is to filter out the sensor noise. Note that t_f changes as the range to the target changes.

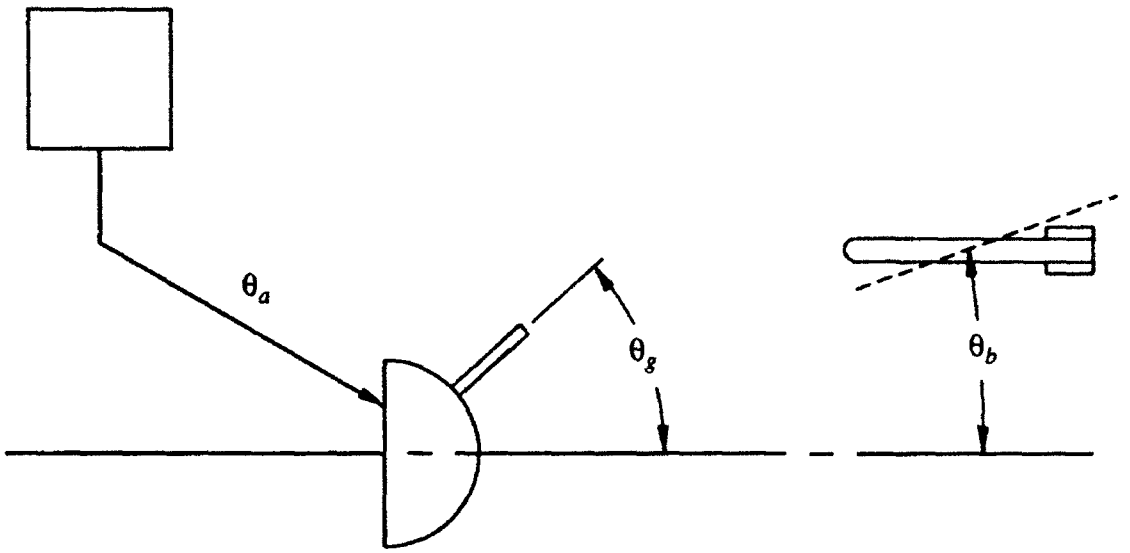

FIGURE 1. PHALANX CIWS ANGLE DIAGRAM

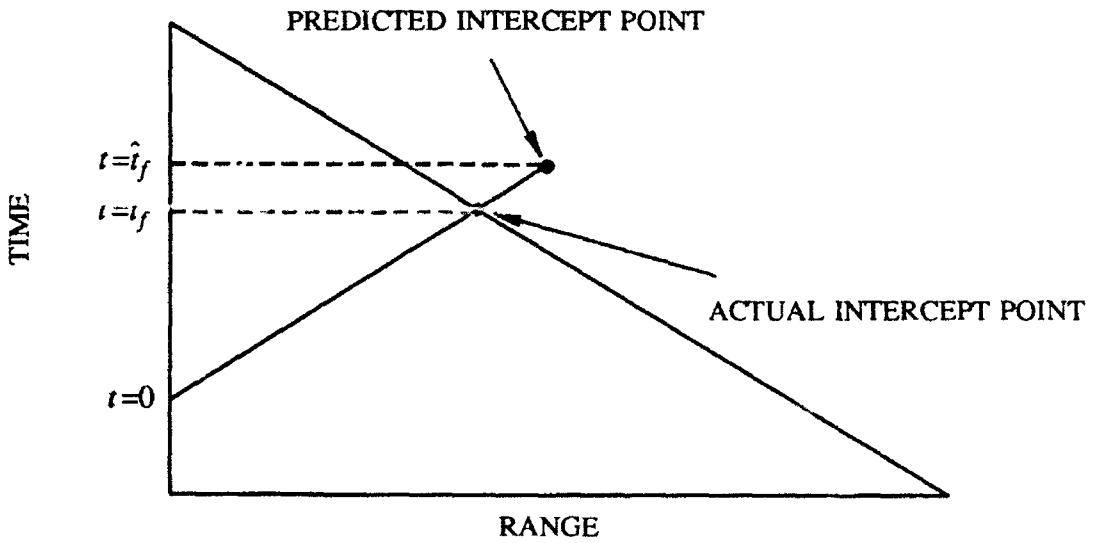

FIGURE 2. PHALANX CIWS TIMING DIAGRAM

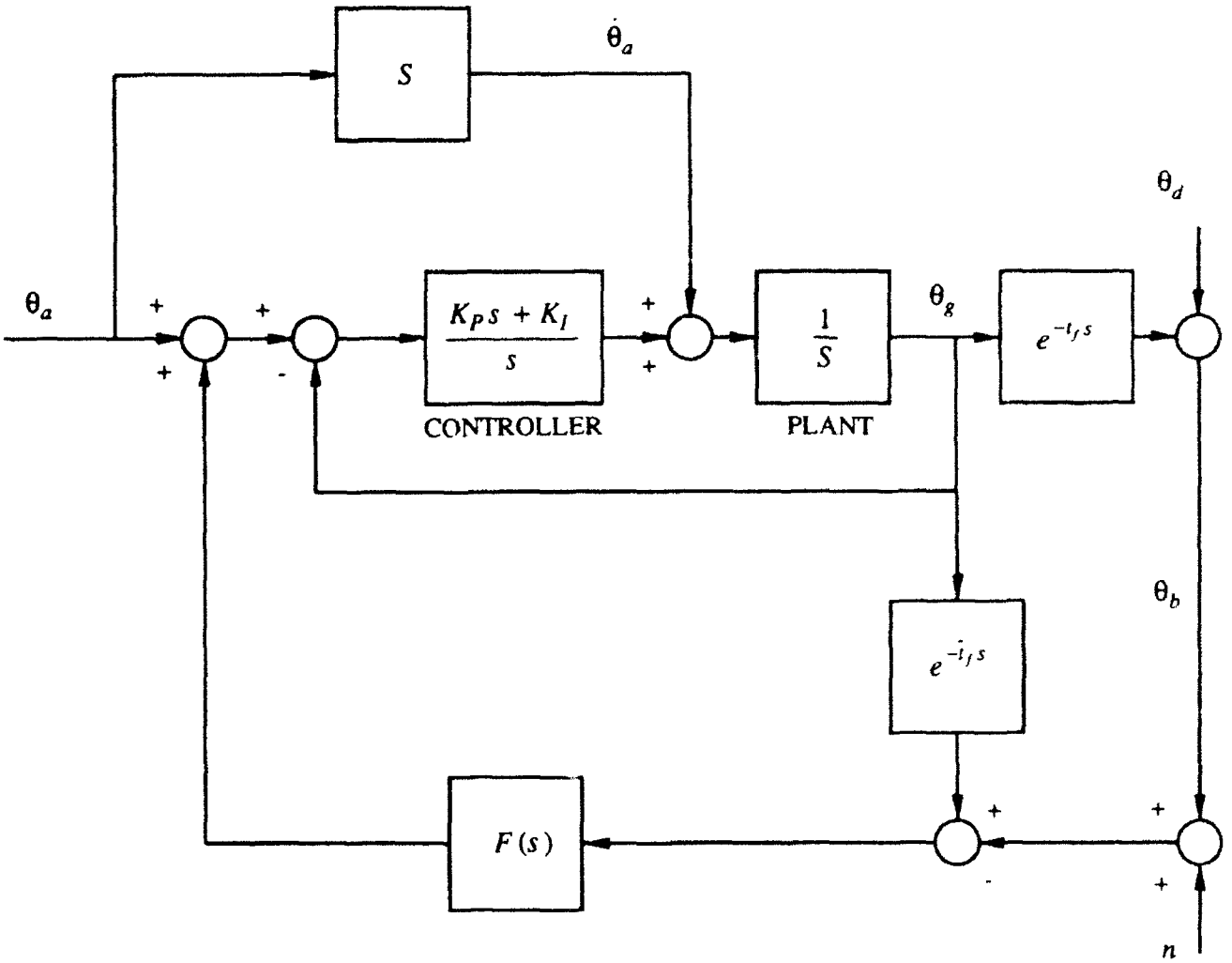

FIGURE 3. PHALANX CIWS AIMING CONTROL SYSTEM

A point to consider is whether this system is a time-varying system. At first glance, because t_f is not fixed, it may be concluded that it is a time-varying system. In an implementation, t_f will change continuously as the target maneuvers, and $\hat{t}_f$ will change at discrete instances as it is recomputed by software within the gun system. Apparently, there is no problem with classifying the system as time-varying. However, there is another point of view. The system may also be classified as a time-invariant adaptive system. If a target is engaged one hour later (or a day later) the system will perform the same; hence, it is time-invariant. The bullet flight time, t_f, may be thought of as a generalized input and $\hat{t}_f$ is then an adaptation parameter computed by system software.

The first thing to do in employing the Small-Gain Theorem is to compute the required system transfer functions. We need the transfer functions $(\theta_b/\theta_a)(s)$, $(\theta_b/\theta_d)(s)$ and $(\theta_b/n)(s)$. These may be computed using Mason's gain rule[4]. We organize the loop gains and path gains. There are three loops.

$$L_1 = -\frac{(K_P s + K_I)}{s^2}$$

$$L_2 = \frac{(K_P s + K_I)}{s^2} e^{-\hat{t}_f s} F(s)$$

$$L_3 = -\frac{(K_p s + K_I)}{s^2} e^{-t_f s} F(s)$$

There are two paths from θ_a to θ_b.

$$P_1^a = \frac{(K_p s + K_I)}{s^2} e^{-t_f s}$$

with associated *loop touching factor* $\Delta_1^a = 1$, and

$$P_2^a = e^{-t_f s}$$

with $\Delta_2^a = 1$. There is one path from θ_d to θ_b. $P^d = 1$ with $\Delta^d = 1 - L_1 - L_2$. The path from n to θ_b has gain

$$P^n = -F(s)\frac{(K_P s + K_I)}{s^2} e^{-t_f s}$$

The loop touching factor is $\Delta^n = 1$. We have that the Mason loop gain is $\Delta = 1 - L_1 - L_2 - L_3$ (there are no *no touching* loops). Now,

$$\frac{\theta_b}{\theta_a}(s) = \frac{P_1^a \Delta_1^a + P_2^a \Delta_2^a}{\Delta}$$

$$= \frac{\left[1 + \frac{K_P s + K_I}{s^2}\right] e^{-t_f s}}{1 + \frac{(K_P s + K_I)}{s^2}\{1 + F(s)[e^{-t_f s} - e^{-\hat{t}_f s}]\}}$$

$$= \frac{(s^2 + K_P s + K_I) e^{-t_f s}}{s^2 + (K_P s + K_I)\{1 + F(s)[e^{-t_f s} - e^{-\hat{t}_f s}]\}} \qquad (1)$$

If $\hat{t}_f = t_f$, then $(\theta_b/\theta_a)(s)$ becomes

$$\frac{\theta_b}{\theta_a}(s) = e^{-t_f s}$$

;i.e., the bullet angle at the target is equal to the aiming angle delayed by t_f seconds (so the aim bias is compensated for) which is what we want. Right away, we see from Equation (1) that the time delay estimation error is attenuated or amplified by F. If $\dot{\theta}_a$ is not used as a control input, then $P_2^a = 0$ and $(\theta_b/\theta_a)(s)|_{\hat{t}_f = t_f}$ becomes

$$\left.\frac{\theta_b}{\theta_a}(s)\right|_{\hat{t}_f = t_f} = \left[\frac{K_P s + K_I}{s^2 + K_P s + K_I}\right] e^{-t_f s} .$$

which is a type zero system and so, only step inputs can be tracked.

The disturbance transfer function is

$$\frac{\theta_b}{\theta_d}(s) = \frac{P^d \Delta^d}{\Delta}$$

$$= \frac{1 + \frac{(K_P s + K_I)}{s^2}\{1 - e^{-\hat{t}_f s} F(s)\}}{1 + \frac{(K_P s + K_I)}{s^2}\{1 + F(s)[e^{-t_f s} - e^{-\hat{t}_f s}]\}}$$

$$= \frac{s^2 + (K_P s + K_I)\{1 - e^{-t_f s} F(s)\}}{s^2 + (K_P s + K_I)\{1 + F(s)[e^{-t_f s} - e^{-t_f s}]\}}$$

$$= 1 - T(s) \tag{2}$$

where

$$T(s) = \frac{F(s)(K_P s + K_I)e^{-t_f s}}{s^2 + (K_P s + K_I)\{1 + F(s)[e^{-t_f s} - e^{-t_f s}]\}} \tag{3}$$

The noise transfer function is

$$\frac{\theta_b}{n}(s) = \frac{P^n \Delta^n}{\Delta}$$

$$= \frac{-F(s)\dfrac{(K_P s + K_I)}{s^2} e^{-t_f s}}{1 + \dfrac{(K_P s + K_I)}{s^2}\{1 + F(s)[e^{-t_f s} - e^{-t_f s}]\}}$$

$$= \frac{-F(s)(K_P s + K_I)e^{-t_f s}}{s^2 + (K_P s + K_I)\{1 + F(s)[e^{-t_f s} - e^{-t_f s}]\}}$$

$$= -T(s) \tag{4}$$

These transfer functions are linear with time delays. Equations (2) and (4) compare to the equation (2.3.3) found in Reference 2.

We next consider the stability of the system. The first task is to assure the stability of the inner loop as if it were a stand-alone system. The transfer function of the inner loop is

$$\frac{\theta_g}{\theta_a} = \frac{K_P s + K_I}{s^2 + K_P s + K_I} \tag{5}$$

For stability, the poles of the inner loop characteristic polynomial $s^2 + K_P s + K_I$ must be in the left half plane. This is done by selecting $K_P > 0$ and $K_I > 0$, which also makes the inner loop a minimum phase system. Note that when $\omega = \sqrt{K_I}$, $\left| \frac{\theta_g}{\theta_a}(j\omega) \right| > 1$.

We use the Small-Gain Theorem to give sufficient conditions for the stability of the overall system. In fact, the conditions will be conservative, which is a consequence of the broad applicability of the Small Gain Theorem, which includes time-varying systems with time delays. Frequency domain conditions will be given because they will be the most useful in conjunction with the noise sensitivity and disturbance rejection conditions. To consider the stability of this system, it will be convenient to redraw the block diagram, Figure 4. Because θ_a and $\dot{\theta}_a$ are inputs to the system, θ_a is restricted such that both $|\theta_a(t)|$ and $|\dot{\theta}_a(t)|$ are bounded. By superposition, the stability of the system is determined by the stability of the system with switch 1 (sw#1) closed and switch 2 (sw#2) open and vice versa. To use the Small-Gain Theorem, we need the closed-loop gain for each of these cases. The system will be stable if the closed-loop gain of the system is less than one. (See Corollary 15, p. 43 of Reference 1.) When sw#1 is closed and sw#2 is open, the loop transfer function is

$$L = F(s)\cdot(e^{-t_f s} - e^{-\hat{t}_f s})\cdot\frac{(K_P s + K_I)}{(s^s + K_P s + K_I)} \tag{6}$$

When sw#2 is closed and sw#1 is open, Figure 4 may be redrawn to look like Figure 5(a). But Figure 5(a) is stable if Figure 5(b) is stable. Figure 5(b) is the same as Figure 5(c). These may be verified e.g, with Mason's rule. Hence, the loop transfer function when sw#2 is closed is again given by Equation (6). By the Small-Gain Theorem, a sufficient condition for the stability of the system is that the loop gain given by Equation (6) is less than one.

The loop gain, Equation (6), is shown in Figure 6. We need the gain from e to the point x_3 to be less than one. Because this is a linear system, we just need to consider what happens when a signal with unit amplitude is input; e.g., $e(t) = \cos(\omega_0 t)$. The signal at point x_1 is $G_1(\omega_0)\cos(\omega_0 t + \phi_1)$ where

$$G_1(\omega) = \left| \frac{K_P j\omega + K_I}{-\omega^2 + K_P j\omega + K_I} \right| \tag{7}$$

and where ϕ_1 is a constant. The gain of e up to x_1 is $G_1(\omega_0)$ (i.e., $\|x_1\| = G_1(\omega_0)$). At x_2 the signal is $G_2(\omega_0)G_1(\omega_0)\cos(\omega_t + \phi_1 + \mu(t))$

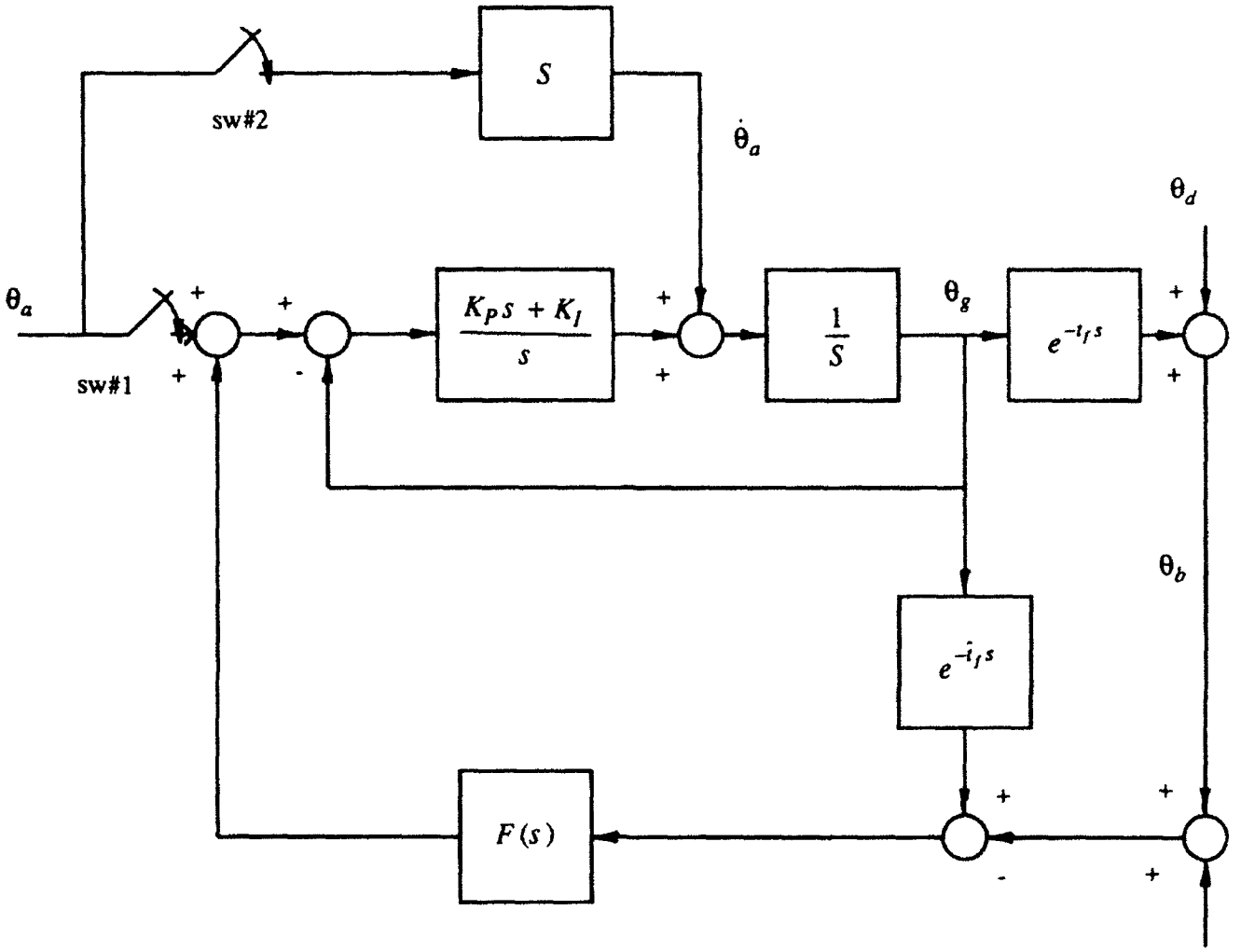

FIGURE 4. BLOCK DIAGRAM FOR STABILITY ANALYSIS

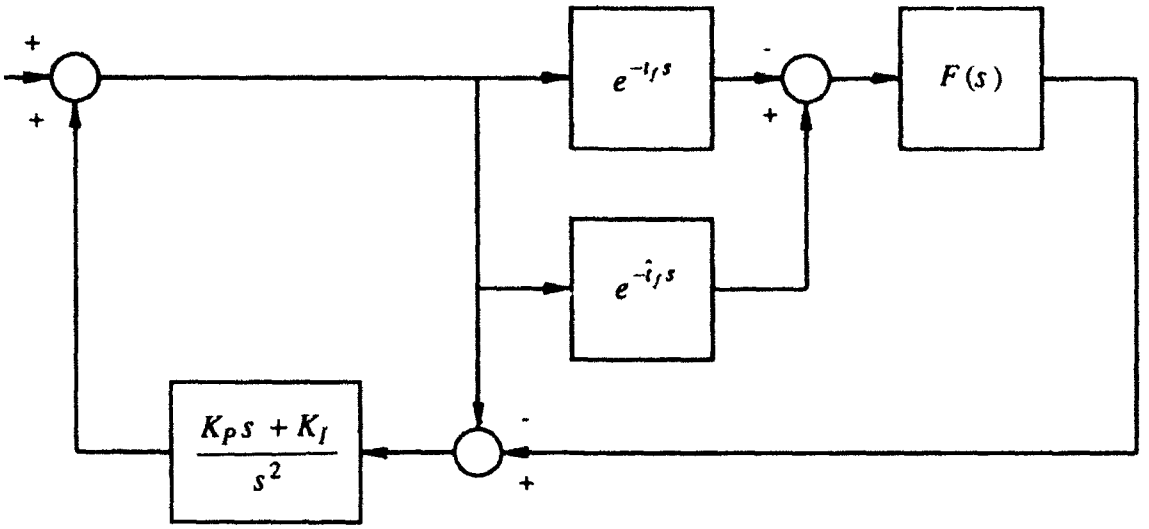

(a)

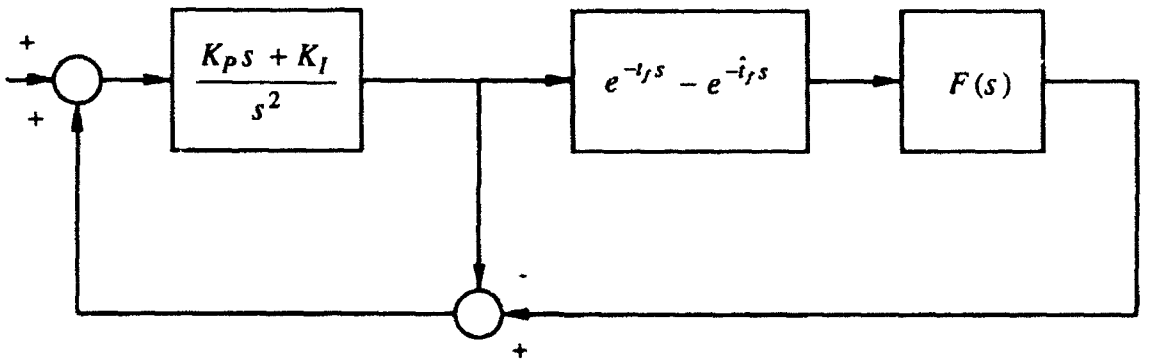

(b)

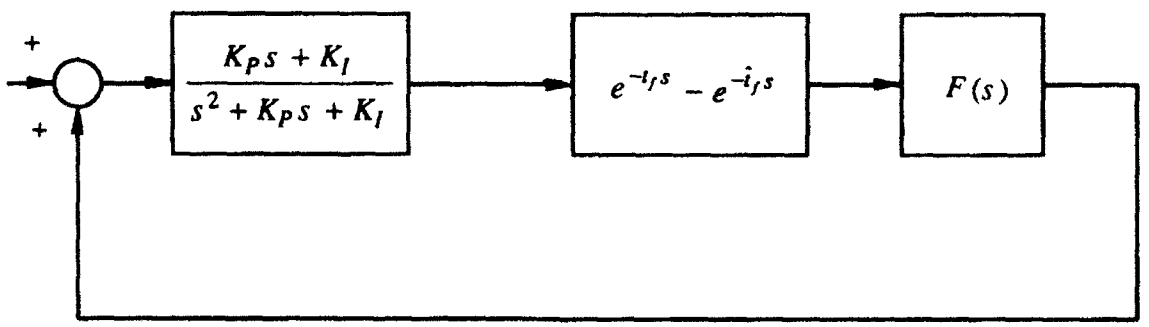

(c)

FIGURE 5. EQUIVALENT BLOCK DIAGRAMS

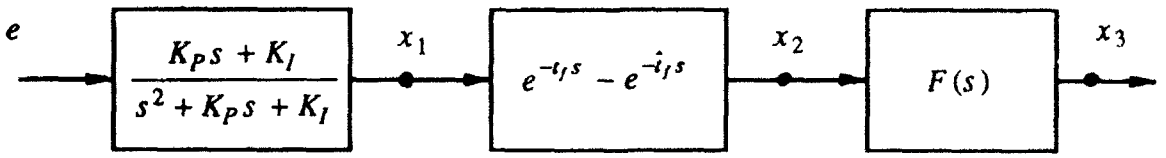

FIGURE 6. LOOP GAIN

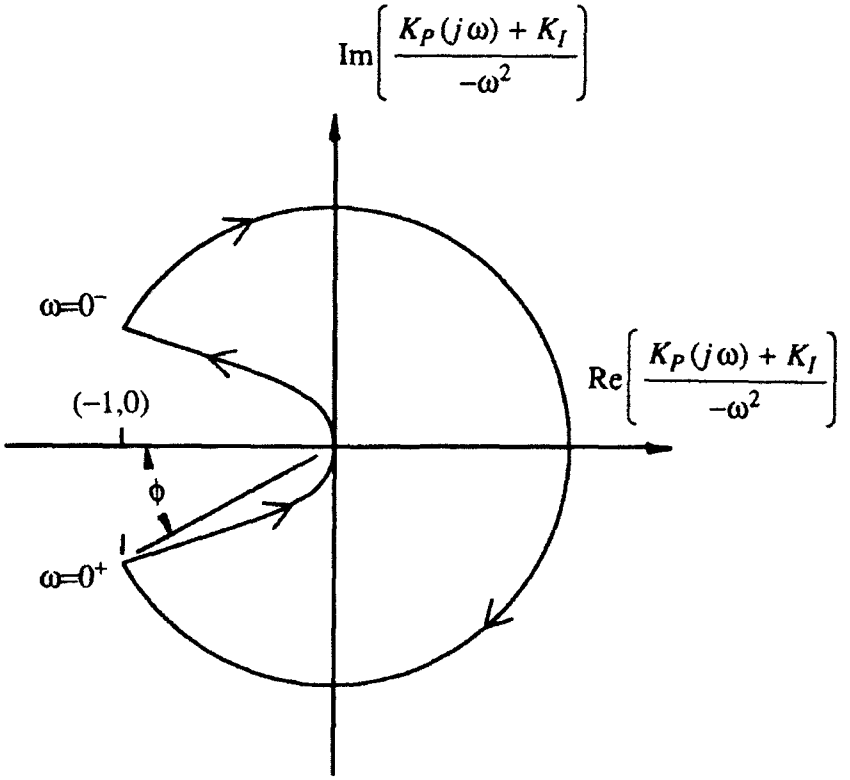

FIGURE 7. NYQUIST PLOT OF $(K_P(j\omega) + K_I)/(-\omega^2)$

where

$$G_2(\omega) = |e^{-t_f j\omega} - e^{-\hat{t}_f j\omega}| = |2 \cdot \sin((t_f - \hat{t}_f)\omega/2)| \tag{8}$$

and where

$$\mu(t) = \text{angle}[e^{-t_f j\omega} - e^{-\hat{t}_f j\omega}] = \frac{(t_f - \hat{t}_f)\omega + \pi}{2} \tag{9}$$

is a time-varying phase shift. Because $\mu(t)$ is time varying, the signal at x_2 is an exponentially modulated signal. It is not a signal with frequency ω_0, rather it has a spectrum centered about the carrier frequency ω_0. Its bandwidth may be computed by Carson's rule[5]. Let $(t_f - \hat{t}_f)$ have maximum deviation, ϕ_Δ, and maximum frequency, W. The deviation ratio is $\Delta = \frac{1}{2}\phi_\Delta\omega$. By Carson's rule, the bandwidth of the signal at x_2 is $B(\omega_0) = 2 \cdot (\Delta + 1) \cdot W$. We will assume that the spectrum of x_2 is entirely contained within the bandwidth $B(\omega_0)$ on either side of the carrier frequency ω_0. The gain of the signal at x_2 is $G_2(\omega_0) \cdot G_1(\omega_0)$, the same as it would be if $\mu(t)$ were a constant. We compute the gain at x_3 due to $e(t) = \cos(\omega_0 t)$ as follows:

Compute $B(\omega_0)$ and find

$$G_3(B(\omega_0)) = \max_{\omega_0 - B(\omega_0) \le \omega \le \omega_0 + B(\omega_0)} |F(j\omega)| \tag{10}$$

then the gain at x_3 is bounded by

$$G(\omega_0) = G_3(B(\omega_0)) \cdot G_2(\omega_0) \cdot G_1(\omega_0) \tag{11}$$

The loop gain for the overall closed loop system is bounded by

$$G = \sup_{\omega_0} G(\omega_0) \tag{12}$$

We take a brief look at the size of the loop gain. For higher frequencies, looking at Equation (11), things should be fine because $G_1(\omega)$ goes to zero, $G_2(\omega)$ is less than two and the filter is selected such that $G_3(\omega)$ is bounded. At low frequencies, $G_1(\omega)$ is about one and $G_2(\omega)$ approaches zero. The product of $G_1(\omega)$ and $G_3(B(\omega))$ must be less that one half before $G_2(\omega)$ reaches two for the first time. For faster inner loop dynamics, $G_1(\omega)$ will break at a higher frequency, so that $|t_f - \hat{t}_f|$ must be smaller; hence, a more accurate $\hat{t}_f$ is required. Suppose that the filter is a low

pass filter of the form $F(s) = A/(s + A)$. Again, looking at Equation (8), if the filter breaks at a higher frequency, $\hat{t}_f$ must be more accurate. Also, for this type of filter, if W is larger $G_3(B(\omega))$ will drop at a higher frequency, so that a more accurate $\hat{t}_f$ is required. (See Equation (10).)

Consider the disturbance and noise. As mentioned in the Introduction, disturbances are a factor at low frequencies, while noise is a factor at high frequencies. Looking at Equations (2) and (4), disturbance rejection (at low frequencies) and low noise sensitivity (at high frequencies) are achieved if $\| T(j\omega) \|$ is small at high frequencies and $T(s) \simeq 1$ at low frequencies. If the system is run open-loop; i.e., $F(s) = 0$, the system will not be susceptible to noise; however, we need the feedback to reduce the impact of the disturbance to the system. At low frequencies $e^{t_f j\omega} \simeq 1$ and because $\omega(\hat{t}_f - t_f) \simeq 0$, we have that $e^{-\hat{t}_f(j\omega)} - e^{-t_f(j\omega)} \simeq 0$. Hence, at low frequencies

$$T(j\omega) \simeq \frac{F(j\omega)(K_P j\omega + K_I)}{-\omega^2 + (K_P j\omega + K_I)} \simeq F(j\omega)$$

so, $F(j\omega)$ close to one at low frequencies gives better disturbance rejection. Again, suppose the filter is of the form $F(s) = A/(s + A)$. We see from Equations (2) and (4) that if F breaks at a higher frequency there is better disturbance rejection, while F breaking at a lower frequency reduces sensitivity to noise. A design example will be presented later to clarify this discussion.

NYQUIST STABILITY WITH A CONJECTURE

The Nyquist stability conditions will be used in this section to analyze the closed-loop stability of the system. To handle the time-varying nature of this system, the following conjecture will be accepted. Let T be large enough so that all conceivable t_f, $\hat{t}_f$ are in $[0,T]$. If the system is stable for all fixed (time invariant) t_f, $\hat{t}_f \in [0,T]$, then the system is stable for time varying t_f, $\hat{t}_f$ so long as they remain in the interval $[0,T]$. We do not mean that this conjecture could be proven (as counter-examples exist), rather we want to find some conditions which would be necessary.

Equation (1) has

$$\frac{\theta_b}{\theta_a}(s) = \frac{(s^2 + K_P s + K_I)e^{-t_f s}}{s^2 + (K_P s + K_I)\{1 + F(s)[e^{-t_f s} - e^{-\hat{t}_f s}]\}}$$

$$= e^{-t_f s} + \frac{(K_P s + K_I)F(s)[e^{-(t_f + \hat{t}_f)s} - e^{-2t_f s}]}{s^2 + (K_P s + K_I)\{1 + F(s)[e^{-t_f s} - e^{-\hat{t}_f s}]\}}$$

$$= e^{-t_f s} + F(s)\frac{\frac{(K_P s + K_I)}{s^2}[e^{-(t_f + \hat{t}_f)s} - e^{-2t_f s}]}{1 + \frac{(K_P s + K_I)}{s^2}\{1 + F(s)[e^{-t_f s} - e^{-\hat{t}_f s}]\}} \tag{13}$$

If $\hat{t}_f = t_f$, the second term in Equation (13) would be zero and $(\theta_b/\theta_a)(s)$ would be a stable transfer function. Consider the stability of the second term. We need the zeros of

$$1 + \frac{(K_P s + K_I)}{s^2}\{1 + F(s)(e^{-t_f s} - e^{-\hat{t}_f s})\} \tag{14}$$

to be in the left half plane. First, the Nyquist plot of the first factor $(K_P s + K_I)/s^2$ is drawn. See Figure 7. The phase margin is ϕ and there is infinite gain margin. The second factor of Equation (14) is of the form $(1 + \varepsilon)$ with $\varepsilon = F(s)(e^{-t_f s} - e^{-\hat{t}_f s})$. If this term has a phase angle of less than ϕ, the closed-loop system will be stable. A sufficient condition for this is

$$|\sin^{-1}(\varepsilon)| < \phi \tag{15}$$

Equation (15) presents a tradeoff between the error in the flight time estimation error and the filter $F(s)$. That is, wider filter bandwidth requires more accurate $\hat{t}_f$.

DESIGN EXAMPLE

The results presented in the PHALANX CIWS Aiming model section are illustrated by an example. The inner loop stability and performance, overall system stability, disturbance rejection and sensi-

tivity to noise are considered. First, proportional and integral gains K_P and K_I are selected for inner loop stability and performance. We select K_P and K_I so that the two inner loop closed-loop poles are evenly spaced on a half circle of radius 10 in the left half plane. This gives $K_P = 17.33$ rad and $K_I = 100.0$ rad/sec. These poles determine the reaction performance of θ_g to θ_a.

We choose the filter to be a first-order low pass filter,

$$F(s) = \frac{A}{(s + A)} \quad . \tag{16}$$

The pole of $F(s)$ is selected so that the filter breaks at a higher frequency than the disturbance frequency band and at a lower frequency than the noise frequency band. With this choice of $F(s)$, Equation (3) becomes

$$T(s) = \frac{A \cdot (K_P s + K_I) \cdot e^{-t_f s}}{(s^2 + K_P s + K_I) \cdot (s + A) + A \cdot (K_P s + K_I) \cdot [e^{-t_f s} - e^{-\hat{t}_f s}]} \tag{17}$$

and Equation (6) becomes

$$L = \frac{A \cdot (e^{-t_f s} - e^{-\hat{t}_f s}) \cdot (K_P s + K_I)}{(s + A) \cdot (s^2 + K_P s + K_I)} \quad . \tag{18}$$

We want to compute the maximum possible bullet flight time estimation error that maintains stability of the overall closed-loop system. Note that $(t_f - \hat{t}_f)$ enters into Equation (11) in two places. The difference $(t_f - \hat{t}_f)$ appears in $G_2(\omega_0)$ (See Equation (8).) and in $G_3(B(\omega_0))$ via the bandwidth $B(\omega_0)$. (Thus $B(\omega) = 2 \cdot (\frac{1}{2} \max | t_f - \hat{t}_f | \cdot \omega + 1) \cdot W$.) We set values for A and W, say $A = 1.0$ rad/sec and $W = 1.0$ rad/sec. With this value for W, we find the maximum $| t_f - \hat{t}_f |$ such that the loop gain is less than one. Figure 8 shows loop gain vs. frequency for $| t_f - \hat{t}_f | = 0.29$ sec. The gain is less than one for all frequencies; hence, by the Small-Gain Theorem, the overall closed loop system is stable (for $| t_f - \hat{t}_f | \leq 0.29$).

As stated earlier, if A is larger (the filter breaks at a higher frequency), $\hat{t}_f$ must be more accurate; while if A is smaller $\hat{t}_f$ may be less accurate. Also, a larger W will require a more accurate $\hat{t}_f$; while a smaller W allows a less accurate $\hat{t}_f$. Several test cases are given in Table 1.

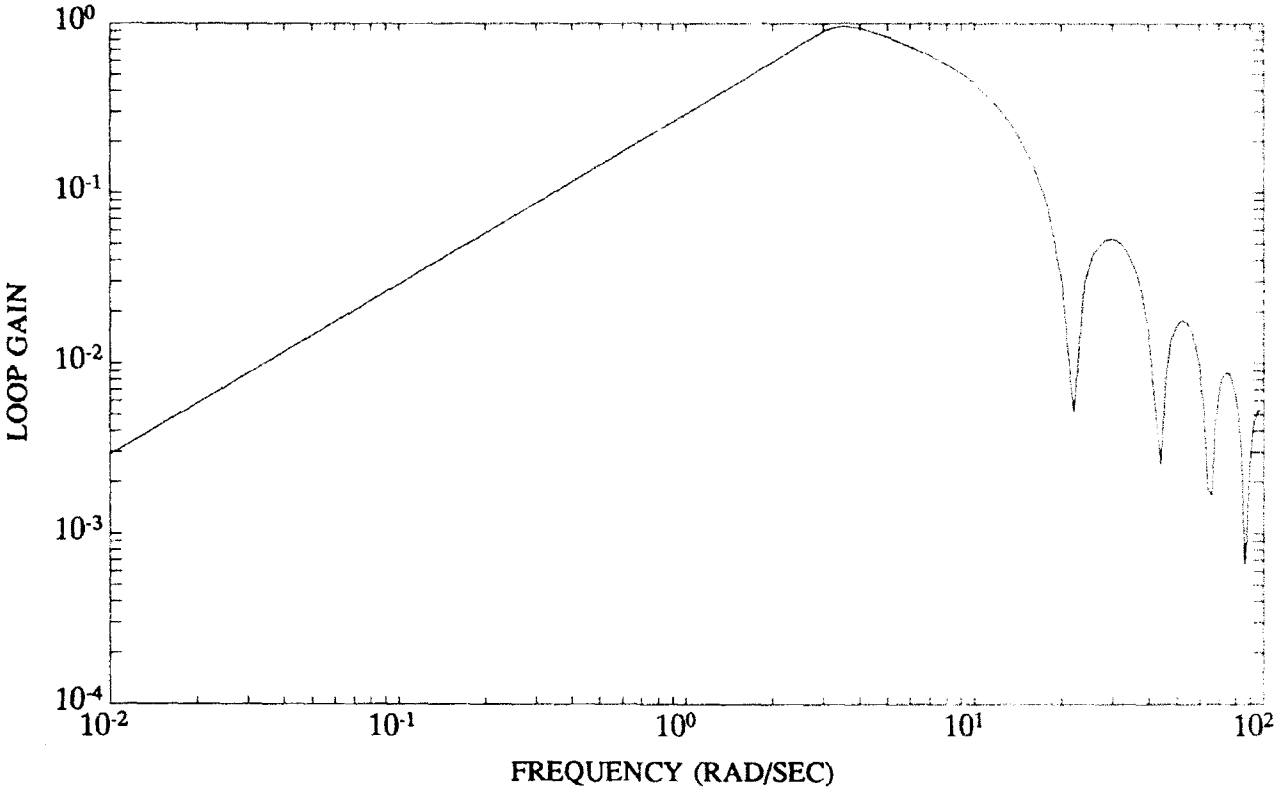

FIGURE 8. LOOP GAIN VS. FREQUENCY

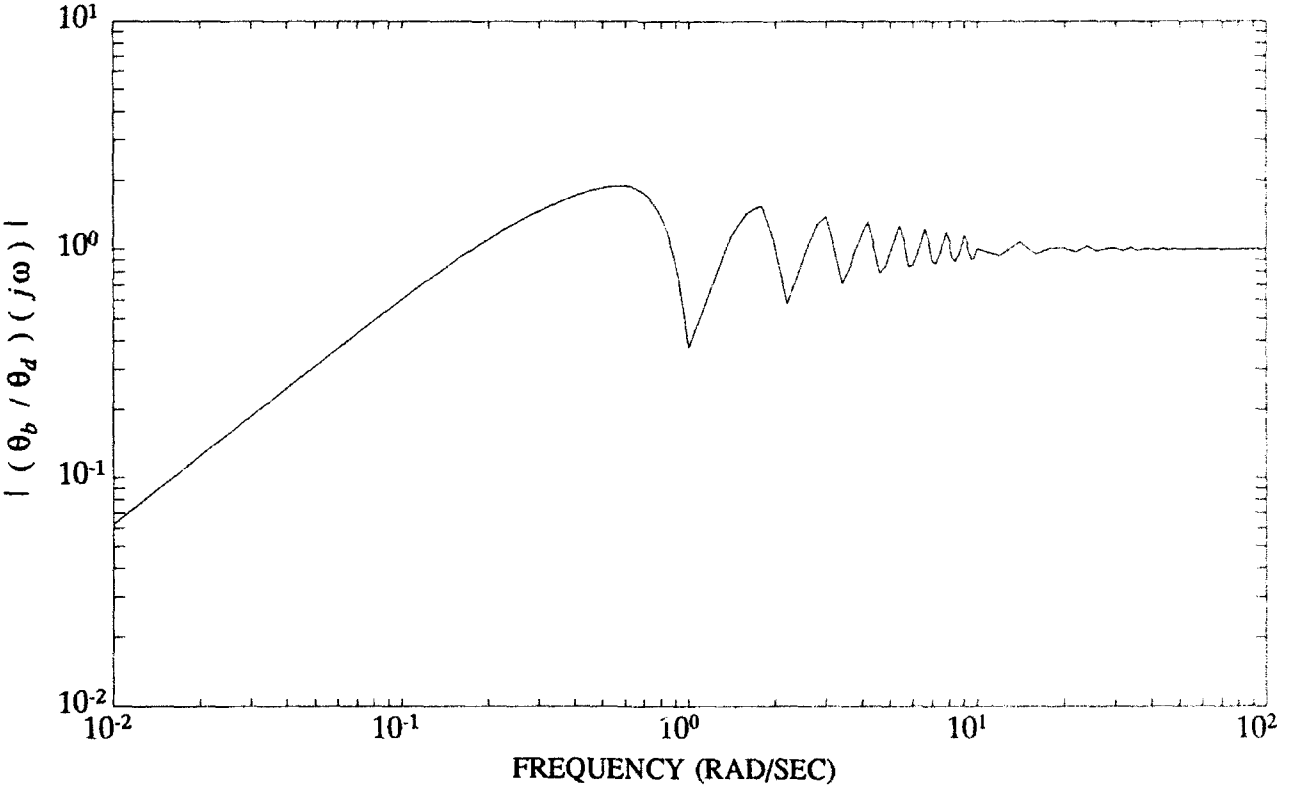

FIGURE 9. DISTURBANCE GAIN VS. FREQUENCY FOR t_f = 5.0 SEC, $\hat{t}_f$ = 5.25 SEC

TABLE 1. MAXIMUM ALLOWABLE $|t_f - \hat{t}_f|$ FOR STABILITY

Maximum $\lvert t_f - \hat{t}_f \rvert$		
A rad/sec	W rad/sec	max$\lvert t_f - \hat{t}_f \rvert$ sec
1.0	0.1	1.09
10.0	0.1	0.129
1.0	1.0	0.29
10.0	1.0	0.10
100.0	1.0	0.069
0.1	10.0	0.32
1.0	10.0	0.068
10.0	10.0	0.068

Finally, we take a look at the disturbance and noise transfer function frequency plots. For the remainder of this report A=1.0 rad/sec and W=1.0 rad/sec. The disturbance and noise transfer functions, Equations (2) and (4), respectively, will be treated as though t_f and $\hat{t}_f$ are constants. Time varying t_f and $\hat{t}_f$ will widen out the disturbance and noise spectrums. Figure 9 shows $|(\theta_b/\theta_d)(j\omega)|$ vs. ω for t_f = 5.0 sec and $\hat{t}_f$ = 5.25 sec. This is about the longest flight time of the bullets. For frequencies less than 0.01 rad/sec, this transfer function has gain less than 0.1; hence, the low frequency disturbances are filtered out and have little effect on the output. Figure 10 shows $|(\theta_b/n)(j\omega)|$ vs. ω for the same t_f and $\hat{t}_f$. For frequencies greater than 40 rad/sec, the gain of this transfer function is less than 0.01; hence, the high frequency noise is filtered out. Finally, we check the disturbance and noise transfer functions for a short bullet flight time. Figures 11 and 12 show $|(\theta_b/\theta_d)(j\omega)|$ and $|(\theta_b/n)(j\omega)|$ vs. frequency, respectively, for t_f = 1.25 sec and $\hat{t}_f$ = 1.0 sec. These represent approximately the shortest bullet flight time. Again, the low frequency disturbances and high frequency noise are filtered out. Of course, Table 1 may be used the other way around; i.e., given a maximum $|t_f - \hat{t}_f|$, A and W may be selected.

Looking at Figures 9 and 11, it seems that $|(\theta_b/\theta_d)(j\omega)|$ drops below 0.1 at too low of a frequency. We would like to get the curves in these figures to drop down at higher frequencies. There is a physical limitation, however. From Figure 3, it is seen that a variation in the disturbance cannot be immediately detected - there is a time delay of t_f seconds. This can also be seen from Equations

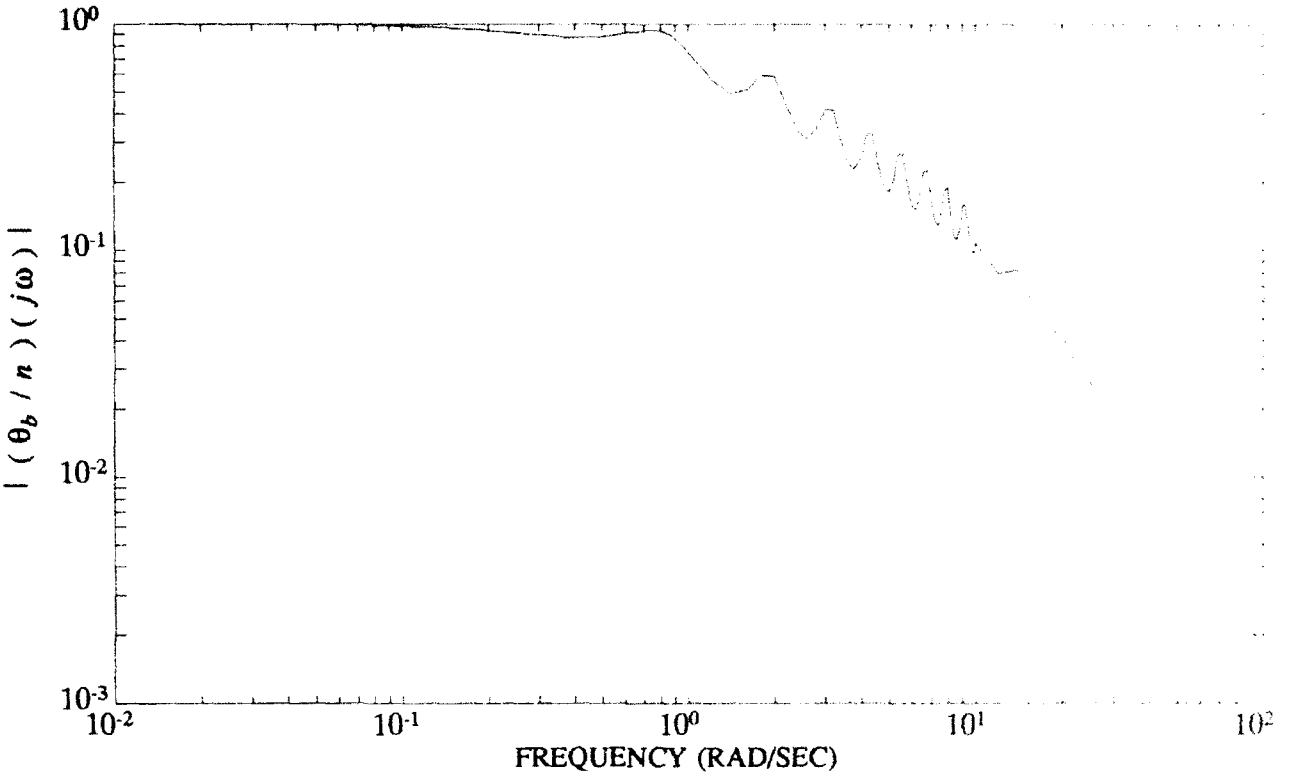

FIGURE 10. NOISE GAIN VS. FREQUENCY FOR t_f = 5.0 SEC, $\hat{t}_f$ = 5.25 SEC

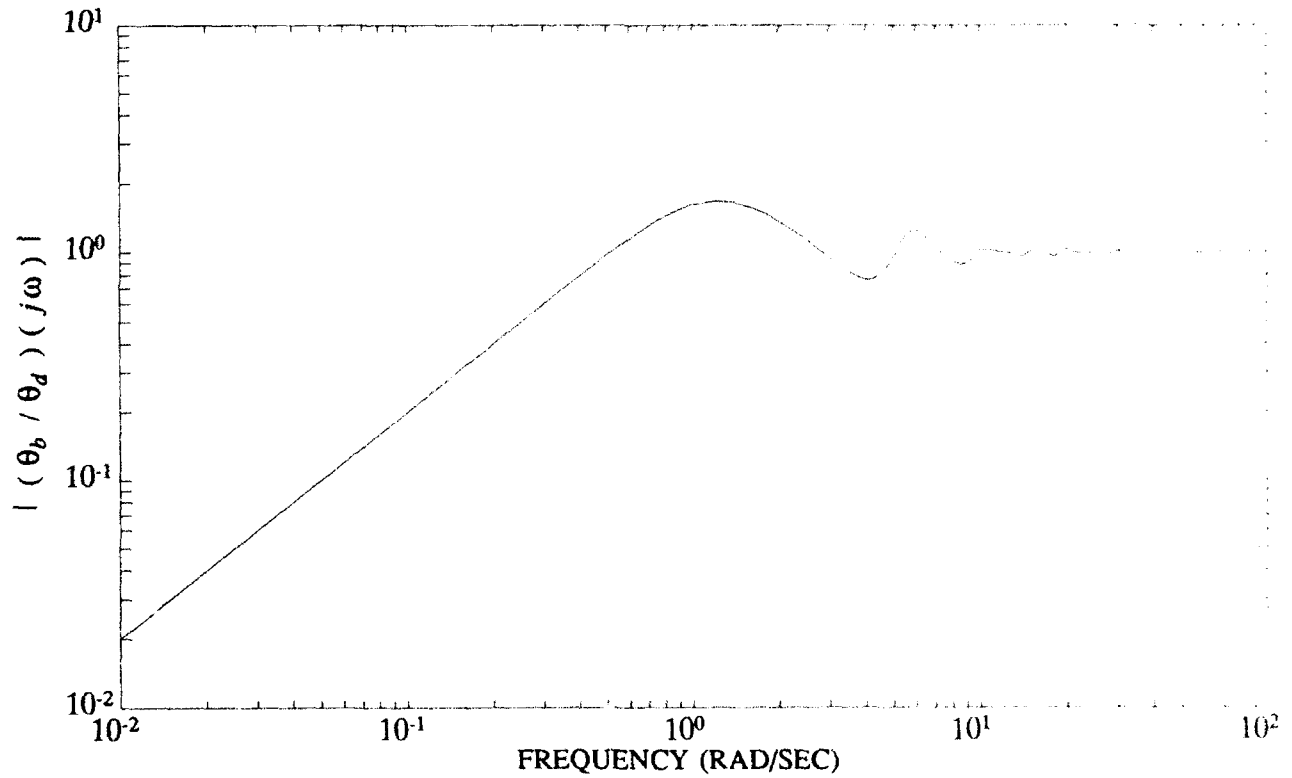

FIGURE 11. DISTURBANCE GAIN VS. FREQUENCY FOR t_f = 1.25 SEC, $\hat{t}_f$ = 1.0 SEC

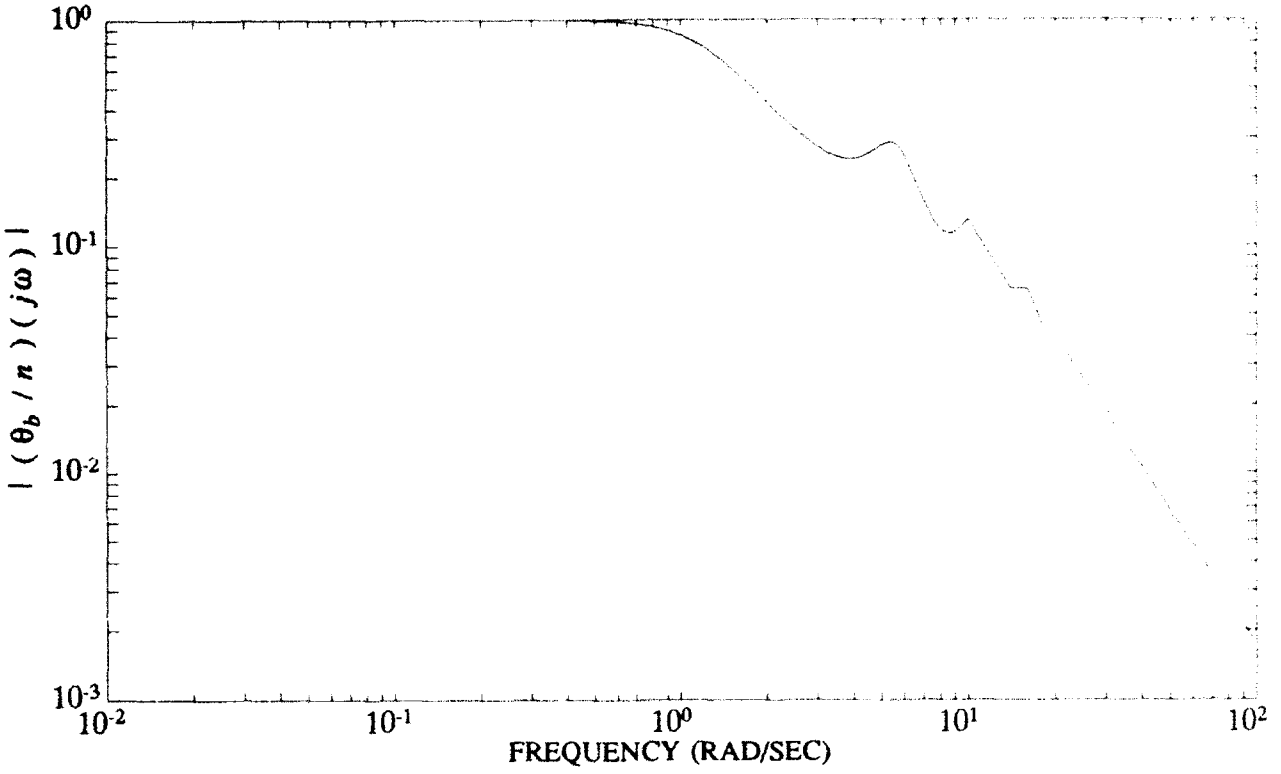

FIGURE 12. NOISE GAIN VS. FREQUENCY FOR t_f = 1.25 SEC, $\hat{t}_f$ = 1.0 SEC

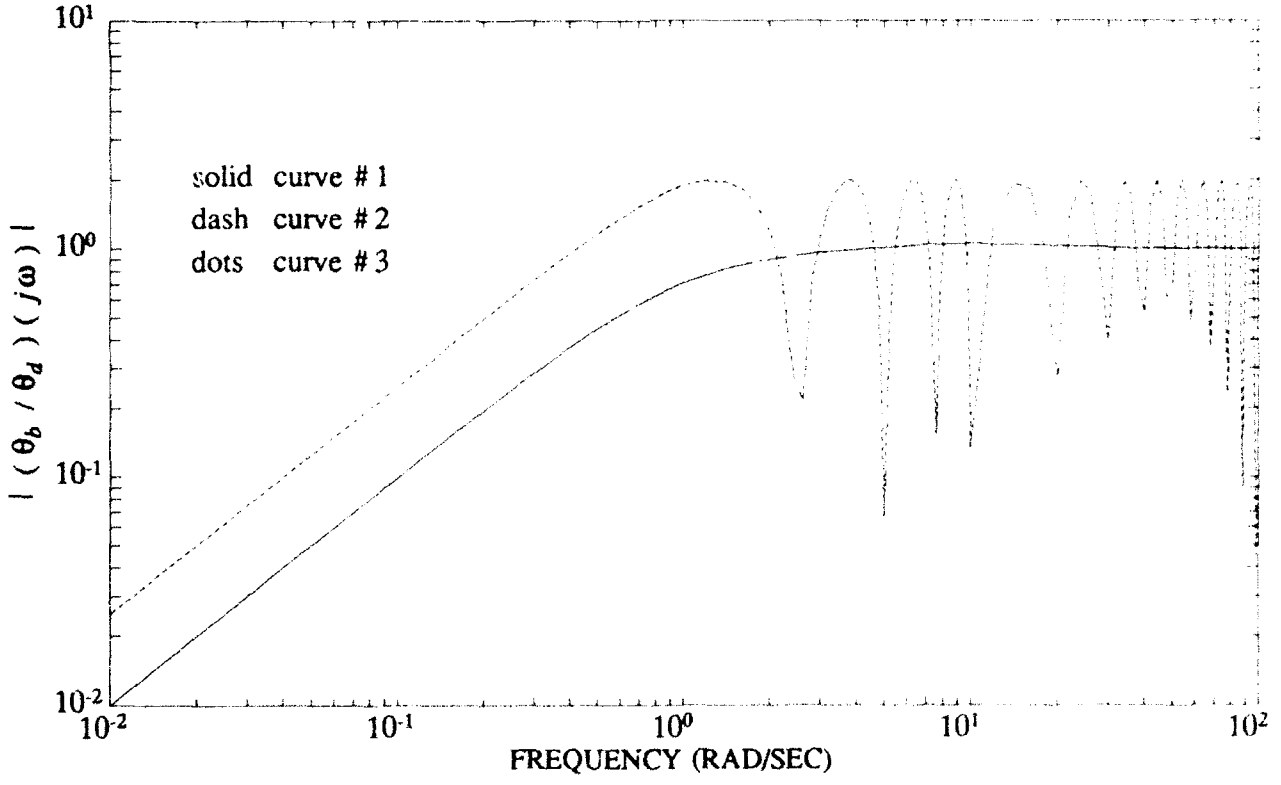

FIGURE 13. DISTURBANCE GAIN LIMITATIONS VS. FREQUENCY

(2) and (17). For $|(\theta_b/\theta_d)(j\omega)|$ to approach zero, $T(j\omega)$ must approach one in magnitude *and* angle. The factor $e^{-jt_f\omega}$ in Equation (17) adds phase lag. We further illustrate this situation in Figure 13. There are three curves, the first is $|1 - (K_P(j\omega) + K_I)\cdot A / ((-\omega^2 + K_P(j\omega) + K_I)\cdot(j\omega + A))|$ vs. ω. This is a plot of the disturbance gain with $t_f = \hat{t}_f = 0$ (and the other parameters as before.) This plot represents the ideal case of disturbance rejection, from the point of view of the physical limitation; i.e., the aim bias is instantaneously fed back. If K_P and A were increased, the break would be at a higher frequency. The second curve in Figure 13 is $|1 - e^{-j\omega t_f}|$ vs. ω with $t_f = 2.5$ sec. This is an average bullet flight time. This represents the physical limitation due to time delay of how fast the disturbance transfer function may approach zero as $\omega \rightarrow 0$. The third curve is a plot of $|(\theta_b/\theta_d)(j\omega)|$ vs. ω with $t_f = \hat{t}_f = 2.5$ sec, so that there is no estimation error. This curve has the combined effects of the first two curves. Hence, the third curve breaks at a lower frequency than either of the first two curves. The first two curves may be thought of as representing the limit of the disturbance rejection performance of the gun aiming control system.

CONCLUSION

The analysis presented in this report provides new insights into the stability characteristics of the aim bias compensation function of the PHALANX CIWS Block 1. Also, tradeoffs between the competing design goals of stability, disturbance rejection (e.g. aim bias compensation) and sensitivity to feedback noise are presented.

The aiming control system is a linear system with a time-varying time delay. The aiming control system features an inner feedback loop servomechanism to aim the gun and an outer loop to null out any aim bias. The time delay results from feeding back the bullet angle at the target through the outer loop. Since the bullet flight time changes, the time delay is time-varying. The Small-Gain theorem may be used to give sufficient stability conditions. The Small-Gain theorem and the noise and disturbance transfer functions are used to analize design tradeoffs. Faster inner loop dynamics, a noise filter with wider bandwidth or a higher frequency in the time delay estimation error signal will result in a less stable system. The filter in the outer loop regulates the disturbance rejection and noise filtering bandwidths. Since the noise and disturbance transfer function must sum to one, more noise filtering results in less disturbance rejection and vice versa. Finally, we have found that the time delay represents a limit to the disturbance rejection bandwidth of the control system.

The insights and design tradeoffs can be used to screen alternatives in the first stages of concept development of new applications or upgraded versions of the PHALANX system. A judicious combination of analytical and experimental analysis will allow a design to be achieved with good balance between stability and responsiveness with a reduced amount of time and effort.

REFERENCES

1. C.A. Desoer and M. Vidyasagar, *Feedback Systems: Input-Output Properties*, Chapter 3, Academic Press, New York, 1975.

2. J.S. Freudenberg and D.P. Looze, *Frequency Domain Properties of Scalar and Multivariable Feedback Systems*, Chapters 1-4, Springer-Verlag, New York, 1988.

3. E.P. Bailey and E.L. Price, "An Analysis of Gun Aim Bias Compensation For The PHALANX CIWS", *FMC Corporation*, King George, VA 22448, May, 1987.

4. J.G. Truxal, *Introductory System Engineering*, page 33, McGraw-Hill, New York, 1972.

5. A.B. Carlson, *Communication Systems: An Introduction to Signals and Noise in Electrical Communication*, page 235, McGraw-Hill, second edition, New York, 1975.

DISTRIBUTION

	Copies
ATTN PMS 413	1
PMS 413TD	1
COMMANDER	
NAVAL SEA SYSTEMS COMMAND	
2531 JEFFERSON DAVIS HWY	
ARLINGTON VA 22242-5160	
ATTN CODE 4L21 (S WILSON)	1
COMMANDER	
PORT HUENEME DIVISION	
NAVAL SURFACE WARFARE CENTER	
PORT HUENEME CA 93043-5007	
ATTN CODE 721 (LCDR SANDERS)	1
COMMANDER	
OPERATIONAL TEST AND	
EVALUATION FORCE	
NORFOLK VA 23511-6388	
ATTN MZ 50 37 (MCCRAY)	1
MZ 50 37 (L SMITH)	1
MZ 4 46 (R BERG)	1
HUGHES MISSILE SYSTEMS CO	
POMONA	
PO BOX 2507	
POMONA CA 91769-2507	
ATTN M H PEE	1
E L PRICE	1
FMC CORPORATION	
EAST COAST ENGINEERING OFFICE	
1 DANUBE DR	
KING GEORGE VA 22485	
ATTN JOE HUDOCK	1
DEFENSE SYSTEMS DIVISION	
ARMAMENT SYSTEMS DEPARTMENT	
LAKE SIDE AVE	
BURLINGTON VT 05402	

	Copies
ATTN GIFT AND EXCHANGE DIVISION	
LIBRARY OF CONGRESS	
WASHINGTON DC 20540	4
DEFENSE TECHNICAL INFORMATION	
CENTER	
CAMERON STATION	
ALEXANDRIA VA 22304-6145	12
INTERNAL DISTRIBUTION:	
A20 (BEUGLASS)	1
B32 (BLAIR)	1
B32 (RICE)	1
B32 (HELMICK)	1
E231	3
E232	2
E281 (SWANSBURG)	1
F107 (ADAMS)	1
F11 (DOSSETT)	1
F41 (STUMP)	1
F43 (KIRKPATRICK)	1
G32 (MCCONKIE)	1
N24 (SERAKOS)	15
N24 (BAILEY)	1
N24 (ADDAIR)	1
N24 (T HENDERSON)	1
N24 (BOYER)	1
N74 (GIDEP)	1

REPORT DOCUMENTATION PAGE

Form Approved
OMB No. 0704-0188

Public reporting burden for this collection of information is estimated to average 1 hour per response, including the time for reviewing instructions, searching existing data sources, gathering and maintaining the data needed, and completing and reviewing the collection of information. Send comments regarding this burden estimate or any other aspect of this collection of information, including suggestions for reducing this burden, to Washington Headquarters Services, Directorate for Information Operations and Reports, 1215 Jefferson Davis Highway, Suite 1204, Arlington, VA 22202-4302, and to the Office of Management and Budget, Paperwork Reduction Project (0704-0188), Washington, DC 20503.

1. AGENCY USE ONLY (Leave blank)	2. REPORT DATE	3. REPORT TYPE AND DATES COVERED
	May 1992	FINAL

4. TITLE AND SUBTITLE
PHALANX CIWS Control System Stability, Aim Bias Compensation, and Noise Sensitivity

5. FUNDING NUMBERS

6. AUTHOR(S)
Demetrios Serakos

7. PERFORMING ORGANIZATION NAME(S) AND ADDRESS(ES)
Naval Surface Warfare Center, Dahlgren Division (Code N24)
Dahlgren, VA 22448-5000

8. PERFORMING ORGANIZATION REPORT NUMBER
NSWCDD/TR-92/243

9. SPONSORING/MONITORING AGENCY NAME(S) AND ADDRESS(ES)

10. SPONSORING/MONITORING AGENCY REPORT NUMBER

11. SUPPLEMENTARY NOTES

12a. DISTRIBUTION/AVAILABILITY
Approved for public release; distribution unlimited.

12b. DISTRIBUTION CODE

13. ABSTRACT (Maximum 200 words)

An aiming control system, which is similar to that in the Block I PHALANX Close-In Weapon System, is considered in this report. An important feature of this control system is that it compensates for any gun aim bias. An aim bias may be caused by variations in the gun, ammunition, or environmental condition. Design issues considered are stability, aim bias compensation, and sensitivity to feedback noise. These are disparate design goals. Design tradeoffs that quantify this disparity are presented. An example is given that illustrates how the analysis developed in this report might be used in a design situation.

14. SUBJECT TERMS
PHALANX, CIWS, Aim Bias, Small-Gain Theorem, Nyquist Stability

15. NUMBER OF PAGES
33

16. PRICE CODE

17. SECURITY CLASSIFICATION OF REPORT	18. SECURITY CLASSIFICATION OF THIS PAGE	19. SECURITY CLASSIFICATION OF ABSTRACT	20. LIMITATION OF ABSTRACT
UNCLASSIFIED	UNCLASSIFIED	UNCLASSIFIED	SAR